A98-31453

ICAS-98-1,3,3

OPTIMIZATION OF SPACE SYSTEM LAUNCHING WITH LIMITATIONS ON FALL ZONES FOR SPENT COMPONENTS

A.S.Filatyev† and O.V.Yanova‡
Central Aerohydrodynamic Institute (TsAGI)
Zhukovsky, Moscow Region, 140160, RUSSIA

Abstract

The problem of optimization of multistage launcher ascent taking account return of spent components to specified fall zones is considered. The topicality of revising nominal ascent trajectories stems from the necessity of reduction of ecological aftereffects of dropping spent components especially when diverse launchers are used for wide nomenclature of payloads in conditions of the contraction of the alienation areas.

The solution is based on the employment of the indirect optimization method of the type of the Pontryagin's maximum principle for branched trajectories. A good convergence of boundary problem solutions is practically invariant with an initial approximation choice owing to the application of the numerical quasi-Newtonian procedure together with parameter continuation and local extremal selection methods. The approach is realized in the automated program complex "ASTER".

It is proven that the restrictions on spent-component fall zones result in a qualitative restructure of the optimal thrust-vector control and in appearance of several local extremals. Some numerical examples are given as concerns optimal injection trajectories with restrictions on fall zones for spent boosters and a nose cover. The possibility of reducing considerably alienation zones for a wide range of orbits to be served with minimum reduction in payloads injected is shown.

†Head of Dept., Flight Dynamics & Control System Div.
‡Senior Scientist Research, FDCS Div.

Introduction

With expansion of the nomenclature of payloads and target orbits and intention to use diverse launchers and their modifications, in particular within the framework of the conversion program, the problem of forming such optimal trajectories that would ensure maximum weight efficiency, provided the spent components return at specified areas to reduce environmental aftereffects of their fall, becomes urgent. The necessity of revising nominal injection trajectories can also be caused by alterations of permissible alienation zones because of changes in the legal status of these territories, rental payments, etc.

The limitation on the spent component fall point leads obligatorily to a qualitative change in the optimal control program for the pitch angle. Indeed, according to the classical results for the optimal spacecraft injection control in the uniform gravitational field[1,2] the introduction of any conditions on the flight range results in the fact that the optimal program of changing the pitch angle tangent is described by a linear-fractional time function rather than by a linear one.

The most comprehensive and objective information on the effectiveness of space transportation systems (STS) can be obtained only on the basis of the complex consideration of all flight phases of STS and its components simultaneously.

In the present work, the problem of injecting a space transportation system with a maximum mass into a specified satellite orbit including

21st ICAS Congress
13-18 September 1998
Melbourne, Australia

limitations on spent component fall zones is solved using the indirect method based on a thorough optimization of branching processes[3] of the Pontryagin's maximum principle type[4]. It is shown that by transferring the conditions from the right ends of trajectories of separated STS components to separation points the reference multi-point boundary problem can be essentially reduced. The investigation is performed for the deterministic nominal flight conditions. A probabilistic scatter of spent component fall points is not considered.

The developed method is implemented in the ASTER program complex[3,5]. To provide the complex operation regularity and independence, the procedures of parameter continuation of the solution and local external selection are used. It allows the known (obtained previously) optimal trajectories to be used as an initial approximation regardless of their "closeness" to the stated problem. The developed ASTER complex interface of Windows type makes specifying the reference data and processing the results obtained maximum convenient. The database of the reference parameters and the calculation results which contains all the variants calculated over the whole operation time of this complex supplements essentially the complex.

The investigation results for optimal trajectories of injecting multi-stage launch vehicles, when spent first- and second-stage boosters and nose covers are dropped at specified points, are presented as the application of the developed method and the program complex to the solution of practical problems of rocket dynamics. The requirement to reduce the spent STS component fall zones is one of the main conditions of providing an admissible safety level and environmental friendliness of space flights. The optimal control laws allow the requirements for spent components fall regions to be satisfied in a wide range of orbit parameter values almost without reducing the payload to be injected. The optimal control programs with consideration for limitations on trajectory branches ensure a new quality for advanced STS and those used at the present time: the capability of direct (without maneuvers to change the orbit plane) injection into orbits in a wide range of inclinations with retention of or even with reduction in the standard spent component fall zones.

1. Problem statement

The trajectory of inserting a space vehicle into an orbit is shown schematically in Fig. 1, where s_1^1 is the start point, s_1^n is a point of reaching a specified orbit, $s_1^j, 2 \le j \le n-1$,are points of separating spent components, $s_2^j, 3 \le j \le n$, are points of falling spent components to the Earth, b_i^j is a continuous trajectory branch between points s_i^j and s_i^{j+1}.

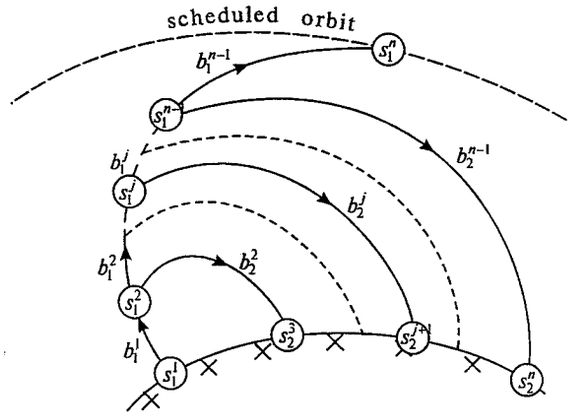

Figure 1: *Branched insertion trajectory.*

In arcs b_1^j, $1 \le j \le n$-1, which form the main branch, the state equations are described in the general form as follows

$$\begin{aligned} \dot{\mathbf{x}}_1^j &= \mathbf{f}_1^j\left(\mathbf{x}_1^j, m_1^j, \mathbf{u}_1^j, t\right) \quad t \in [\tau_1^j, T_1^j] \\ \dot{m}_1^j &= \mu_1^j \end{aligned}, \quad (1)$$

where $\mathbf{x}_1^j$ is the state vector, $\mathbf{u}_1^j$ is the control vector, t is the time, m_1^j is the mass, μ_1^j is the mass flow rate. In general, m_1^j and μ_1^j may be vectors with components for different types of engines.

Assume that dropped structural components (side branches $b_2^j, 2 \le j \le n-1$) move in nominal flight conditions (without accidental disturbances) under determinate control and the

state vector $\mathbf{x}_2^j$ and mass m_2^j on the branch b_2^j are governed by equations

$$\dot{\mathbf{x}}_2^j = \mathbf{f}_2^j(\mathbf{x}_2^j),\ 2 \le j \le n-1$$
$$\dot{m}_2^j = 0, \quad t \in \left[\tau_2^j, T_2^j\right] \qquad (2)$$

At points $s_1^j,\ 2 \le j \le n-1$, the state vectors are taken to be continuous

$$\mathbf{x}_1^{j-1}(T) - \mathbf{x}_1^j(\tau) = 0,\ \mathbf{x}_1^j(\tau) - \mathbf{x}_2^j(\tau) = 0, \qquad (3)$$

and the whole mass is kept constant

$$m_1^{j-1}(T) - m_1^j(\tau) - m_2^j(\tau) = 0. \qquad (4)$$

The mass of dropped components is assumed to be specified:

$$m_2^j,\ 2 \le j \le n-1,\ \textit{is fixed}. \qquad (5)$$

The moments $T_1^{j-1} = \tau_1^j = \tau_2^j,\ 2 \le j \le n$, of the trajectory branching are defined by scalar conditions

$$Q^j\left(\mathbf{x}_1^{j-1}(T), m_1^{j-1}(T)\right) = 0,\ \ 2 \le j \le n-1. \qquad (6)$$

The staging point is generally determined by the condition of attaining a specified mass m_{sp}

$$Q^j \equiv m_1^{j-1}(T) - m_{sp} = 0 \qquad (7)$$

and the nose cover release moment depends on the intersection of a conditional boundary of the dense atmospheric layers which is defined by a function of the flight velocity v and altitude h

$$Q^j\left(v(T_1^{j-1}), h(T_1^{j-1})\right) = 0. \qquad (8)$$

Start conditions and conditions of attaining a specified orbit are assigned at points s_1^1 ($t=t_i$) and s_1^n ($t=t_f$).

Let require that dropped components fall at a specified point, i.e. a radius-vector at a fall point:

$$\mathbf{r}(T_2^j)\ \textit{is fixed}. \qquad (9)$$

The functional to be minimized is the mass of expendable fuel

$$\mathbf{\Phi} \equiv m\left(s_1^1\right) - m\left(s_1^n\right). \qquad (10)$$

3. Maximum principle conditions

The optimization problem for space vehicle insertion with some limitations on fall points for spent STS components is solved by the indirect method of optimizing branched trajectories of the type of the Pontryagin's maximum principle. A specific feature of this problem is displayed only in the expression for the transversality conditions at the branching points $\left\{s_1^j,\ 2 \le j \le n-1\right\}$ and at the ends of side branches $\left\{s_2^j,\ 3 \le j \le n\right\}$.

Let introduce the following notations for the adjoint variables on branch b_i^j:

$\mathbf{P}_i^j$ is the adjoint vector corresponding to radius vector $\mathbf{r}_i^j$,

$\mathbf{S}_i^j$ is the adjoint vector corresponding to velocity vector $\mathbf{v}_i^j$,

$P_{m\,i}^j$ is the adjoint variable (or a vector) corresponding to mass m_i^j and

$\mathcal{H}_i^j$ is the Hamiltonian.

In accordance with[3], we obtain for the state conditions (3) to (6) and (9) and the functional (10) the following transversality conditions.

At points $\left\{s_1^j,\ 2 \le j \le n-1\right\}$ we have:

$$\mathbf{P}_1^j = \mathbf{P}_1^{j-1} - \mathbf{P}_2^j - \lambda_{j-1}\left(\frac{\partial Q_1^j}{\partial \mathbf{r}_1^{j-1}}\right)^T,$$

$$\mathbf{S}_1^j = \mathbf{S}_1^{j-1} - \mathbf{S}_2^j - \lambda_{j-1}\left(\frac{\partial Q_1^j}{\partial \mathbf{v}_1^{j-1}}\right)^T, \qquad (11)$$

$$P_{m\,1}^j = P_{m\,1}^{j-1} - \lambda_{j-1}\frac{\partial Q_1^j}{\partial m_1^{j-1}},$$

$$\mathcal{H}_1^j = \mathcal{H}_1^{j-1} - \mathcal{H}_2^j. \qquad (12)$$

Parameters λ_{j-1} in (11) are found from condition (12):

$$\lambda_{j-1}\left[\frac{\partial Q_1^j}{\partial \mathbf{r}_1^{j-1}}\mathbf{v}_1^j + \frac{\partial Q_1^j}{\partial \mathbf{v}_1^{j-1}}\dot{\mathbf{v}}_1^j + \frac{\partial Q_1^j}{\partial m_1^{j-1}}\dot{m}_1^j\right] = \qquad (13)$$
$$= \left(\mathbf{P}_1^{j-1} - \mathbf{P}_2^j\right)^T \mathbf{v}_1^j + \left(\mathbf{S}_1^{j-1} - \mathbf{S}_2^j\right)^T \dot{\mathbf{v}}_1^j + P_{m1}^{j-1}\dot{m}_1^j.$$

Note to Eq. (13): *Equation (13) is nonlinear with respect to λ_{j-1} because this parameter enters into the optimality conditions for the control* $\mathbf{u}$ *and, accordingly, into* $\dot{\mathbf{v}}_1^j$ *and* $\dot{m}_1^j$. *It can be transformed to the quadratic equation with respect to λ_{j-1} (the only root is satisfied Eq.(13)).*

In a particular case, when the moments of trajectory branching are determined by the attainment of a specified mass (see (7)), the transversality conditions (11) to (13) take the form

$$\begin{cases} \mathbf{P}_1^j = \mathbf{P}_1^{j-1} - \mathbf{P}_2^j \\ \mathbf{S}_1^j = \mathbf{S}_1^{j-1} - \mathbf{S}_2^j \\ P_{m1}^j = P_{m1}^{j-1} - \lambda \end{cases}, \qquad (14)$$

where

$$\lambda = \frac{\left(\mathbf{P}_1^{j-1} - \mathbf{P}_2^j\right)^T \mathbf{v}_1^j + \left(\mathbf{S}_1^{j-1} - \mathbf{S}_2^j\right)^T \dot{\mathbf{v}}_1^j + P_{m1}^{j-1}\dot{m}_1^j}{\dot{m}_1^j} \qquad (15)$$

(see note to Eq. (13)).

In the case (8), the transversality conditions (11) to (13) take the form

$$\begin{cases} \mathbf{P}_1^j = \mathbf{P}_1^{j-1} - \mathbf{P}_2^j - \lambda \dfrac{\partial Q_1^j}{\partial h}\mathbf{e}_R \\ \mathbf{S}_1^j = \mathbf{S}_1^{j-1} - \mathbf{S}_2^j - \lambda \dfrac{\partial Q_1^j}{\partial v}\mathbf{e}_v \\ P_{m1}^j = P_{m1}^{j-1} \end{cases}, \qquad (16)$$

where $\mathbf{e}_R$ is the unit vector in the direction from the gravity center to the separation point s_1^j, $\mathbf{e}_v$ is the unit velocity vector and

$$\lambda = \frac{\left(\mathbf{P}_1^{j-1} - \mathbf{P}_2^j\right)^T \mathbf{v}_1^j + \left(\mathbf{S}_1^{j-1} - \mathbf{S}_2^j\right)^T \dot{\mathbf{v}}_1^j + P_{m1}^{j-1}\dot{m}_1^j}{\dfrac{\partial Q_1^j}{\partial h}\mathbf{e}_R^{\mathrm{T}}\mathbf{v}_1^j + \dfrac{\partial Q_1^j}{\partial v}\mathbf{e}_v^{\mathrm{T}}\dot{\mathbf{v}}_1^j} \qquad (17)$$

(see note to Eq.(13)).

The transversality conditions at the fall points (see (9)) take the form

$$t = T_2^j : \begin{cases} \mathbf{P}_2^j = var, \\ \mathbf{S}_2^j = 0, \\ P_{m2}^j = 0, \\ \mathcal{H}_2^j = \left(\mathbf{P}^T\mathbf{v}\right)_2^j = 0. \end{cases} \qquad (18)$$

4. Boundary-value problem

Use of Pontryagin's maximum principle makes it possible to reduce the initial optimization problem to a multi-point boundary-value problem for the state and adjoint equation sets. In the case of the optimization of the STS ascent trajectory with a single side branch the dimensionality of the boundary-value problem does not exceed the value of (k_1+k_2), where k_1 and k_2 are dimensionalities of equation sets (1) and (2) consequently. Because the right parts of equations (2) are independent of the control the boundary conditions (18) are fulfilled either by means of double integration, i.e., integration of the state system in direct time and the adjoint system in inverse time, or by means of one iteration using the Newton method, thus providing the projection of the boundary conditions from the right ends of side branches on the main branch. In this case, according to Eq. (18), the boundary-value problem dimensionality is reduced to (k_1+2).

To continue the solution in terms of a parameter ε, for example, the optimal solution without the limitation (9) can be considered as a reference solution. It is convenient to introduce the parameter ε as an angular range between a specified vehicle component fall point and an optimal fall point obtained without considering this limitation.

In the reference case with taking account of (18), the adjoint vectors at the right ends of the side branches $\left\{s_2^j\right\}$ are zero and by virtue of the linearity of the adjoint system we obtain a trivial solution on the side branch (see conditions of jump (11), (14) and (16)):

$$\mathbf{P}_2^j(\tau) = \mathbf{S}_2^j(\tau) = P_{m2}^j(\tau) = 0. \qquad (19)$$

5. Local extremals

The conditions of the Pontryagin's maximum principle make it possible to find local extremals only. In order to obtain a solution providing a global optimum, special investigations are required. In the earlier paper[3], some typical

families of local extremals as applied to the problem of aerospace vehicle orbit insertion are demonstrated, a physical nature of their appearance is suggested and the conditions under which they are capable of providing a global extremum are stated.

In the problem considered here, local extremals due to an additional limitation on fall regions for spent components are also expected.

Indeed, assume for definiteness that the 1st stage flies according to the gravitational turn program. Then, the 1st stage trajectory depends, in fact, only on one parameter, namely on the "initial" trajectory angle γ_i realized after a short portion of the vertical ascent and intense pitch turn.

Let the following notations be introduced:

$\gamma_{i\,opt}$ - angle γ_i at which maximum mass $m_{f\,opt}$ is inserted;

$\gamma_{i\,L_I}$ - angle γ_i at which maximum mass $m_{f\,L_I} = m_f(L_I)$ is inserted provided 1st-stage booster falls at a specified distance L_I from the start point;

$\gamma_{i\,L_{max}}$ - angle γ_i at which 1st-stage booster fall distance is maximum $\left(L_I = L_{I\,max}\right.$.

In the region $L_I < L_{I\,max}$, the dependence $\gamma_{i\,L_I} = \gamma_i(L_I)$ is non-single-valued. Let the upper branch of this curve be denoted by $\gamma_i^{up}(L_I)$, and the lower branch by $\gamma_i^{low}(L_I)$ (Fig. 2).

Hence, the dependence of maximum inserted mass on the limitation on 1st-stage booster fall distance is also non-single-valued and has two branches:
$m_{f\,L_I}^{up} = m_f\left(\gamma_i^{up}(L_I)\right)$ and $m_{f\,L_I}^{low} = m_f\left(\gamma_i^{low}(L_I)\right)$, which correspond to two types of local extremals differing in altitude. Depending on relations for $\gamma_{i\,opt}$ and $\gamma_{i\,L_{max}}$, three types of the curve $m_f(L_I)$ are possible (see Fig. 3) which differ in the type of a local extremal providing a global optimum. In the region of $L_I < L_{I\,max}$ the curves $m_f^{up}(L_I)$ and $m_f^{low}(L_I)$ can have an intersection point which is a bifurcation point for optimal trajectories when varying the limitation on the 1st-stage booster fall distance.

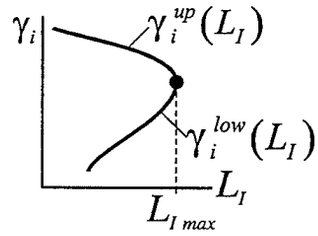

Figure 2: *Qualitative relationship between the initial path angle γ_i and the fall distance L_I.*

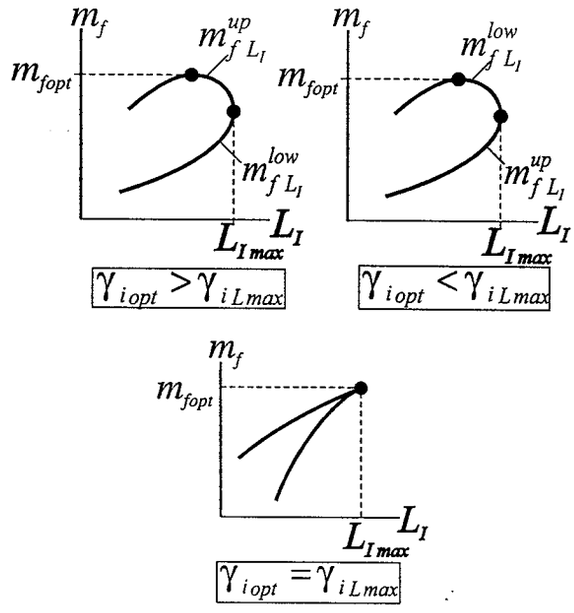

Figure 3: *Different types of the relationship between maximum inserted mass and the limitation on booster fall distance.*

Note that the above qualitative considerations to validate the existence of two types of local extremals are based on the logic of local (small) variations. Therefore, in applying the Pontryagin's maximum principle, which is valid for strong (needle-type) control variations, the second (worse) extremal may not manifest itself (not satisfy the maximum principle conditions). For example, only one, the optimal solution exists for the optimal R-type launcher (see Sec. 6) injection with the limitation on the fall distance of the I-stage booster.

6. Numerical results

To illustrate the method considered above, optimal branched trajectories for insertion of a multi-stage launcher with limitation on spent components fall distance were calculated using the "ASTER" program package [3,5]. Two types ("P" and "R") of launchers are considered.

P-type launcher has 4 stages with initial mass ratios as 1 : 0.35 : 0.10 : 0.03. The limitations on the launcher control and motion are as follows: $|\alpha| \le 5°$ (1st-stage), $|q\alpha| \le 9 \cdot 10^3$ kgf/m^2 (1st- and 2nd-stages), α is the angle of attack, q is the dynamic pressure. The launcher is inserted into a circular orbit with a height of $h_{orb} = 200$ km and nominal inclination of $i_{orb} = 51.6°$, the start point latitude being $\phi = 46°$.

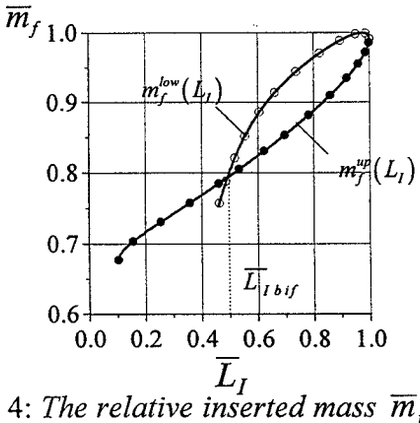

Figure 4: *The relative inserted mass $\overline{m}_f$ vs. the relative 1st-stage booster fall distance $\overline{L}_I$.*

Fig. 4 exemplifies the relative maximum injected mass $\overline{m}_f(\overline{L}_I) = \dfrac{m_f(\overline{L}_I)}{\max\limits_{\overline{L}_I} m_f}$ versus the relative distance of the I-stage booster fall point $\overline{L}_I = L_I / L_{I\max}$. Two types of global extremals and respective optimal pitch angle programs for the bifurcation value of $\overline{L}_I = \overline{L}_{I\,\text{bif}} \approx 0.49$ are shown in Fig. 5.

The capability of reducing considerably fall regions for a spent 1st-stage booster due to the optimization of a three-dimensional launcher maneuver during insertion was investigated for a wide range of orbit inclinations. In particular,

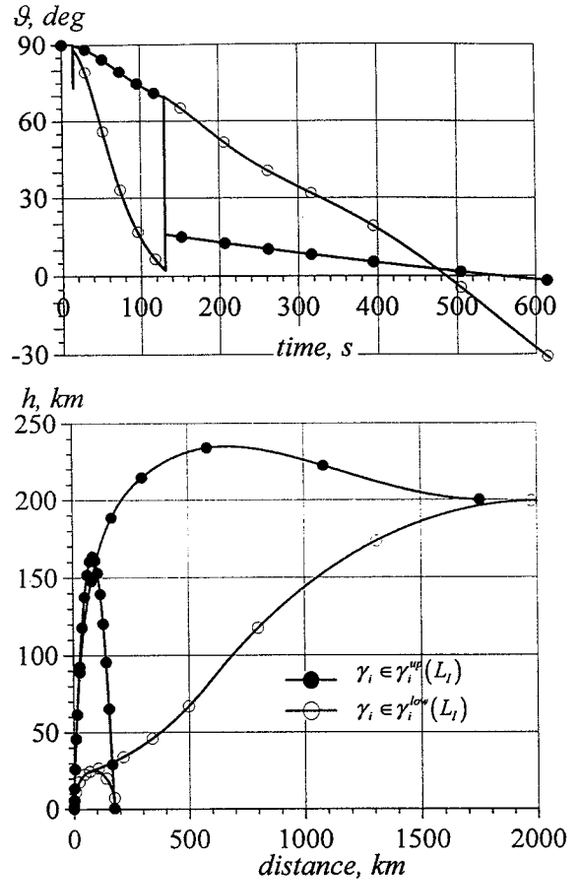

Figure 5: *Optimal pitch control programs and optimal insertion trajectories in the vertical plane for different types of local extremals at the bifurcation point.*

the capability of directing the spent 1st-stage booster to one point is discussed for the range of orbit inclinations of $51° < i_{orb} < 72°$.

The comprehensive analysis of all flight phases using the same criterion ensures, on the one hand, the most complete consideration of specific limitations and, on the other hand, the realization of the best insertion scheme and a maximum weight efficiency.

If a specified fall point is aside from the nominal insertion trajectory trace the optimal launch azimuth is varied so that the insertion portion for the 1st stage be oriented to a specified fall point (Fig. 6).

Upon separation of the 1st-stage, the launcher performs an intense banked turn so as the insertion plane inclination almost coincides with

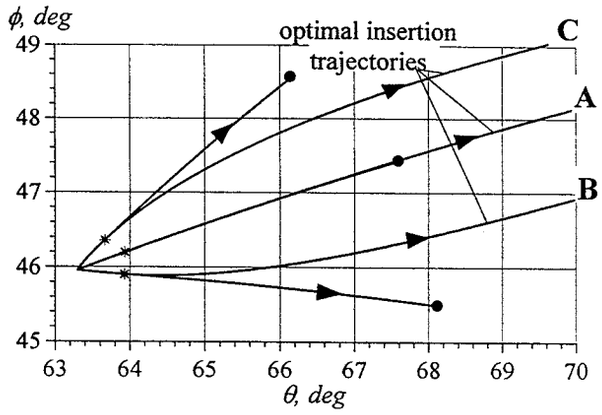

Figure 6: *Optimal launcher trajectories for fixed 1st-stage booster fall points:* **A** *- the fall point is free,* **B**, **C** *- the fall points are fixed,* • *- fall points,* * *- staging points.*

the inclination of the orbit plane, the pitch control program remaining essentially the same (Fig. 7).

If an additional condition is introduced to specify the fall point for a spent 1st-stage booster, this condition causes, of course, some reduction in the mass Δm_f to be inserted. The value of Δm_f is, as a rule, of the 2nd-order infinitesimal with respect to the distance of the specified fall point from the optimal one. (The optimal fall point corresponds to the solution of the problem without the fall point limitation.) Therefore, small deviations of the fall point do not almost affect the inserted mass.

Fig. 8 presents in the geographic coordinates (latitudeϕ vs. longitude θ) level lines for the inserted mass in the case of variations of specified 1st-stage booster fall points at orbit inclinations of $i_{orb} = 51.6°$ and 72.6°. It is seen that the optimal fall point lies near the boundary of the Earth's surface region attained limitedly by the spent 1st-stage booster. This means that the optimal 1st-stage insertion trajectory providing the delivery of maximum payload to the orbit is close to the trajectory which is optimal by the criterion of the 1st-stage booster range.

It is worthy of note that the requirement on falling the 1st-stage booster in one or several

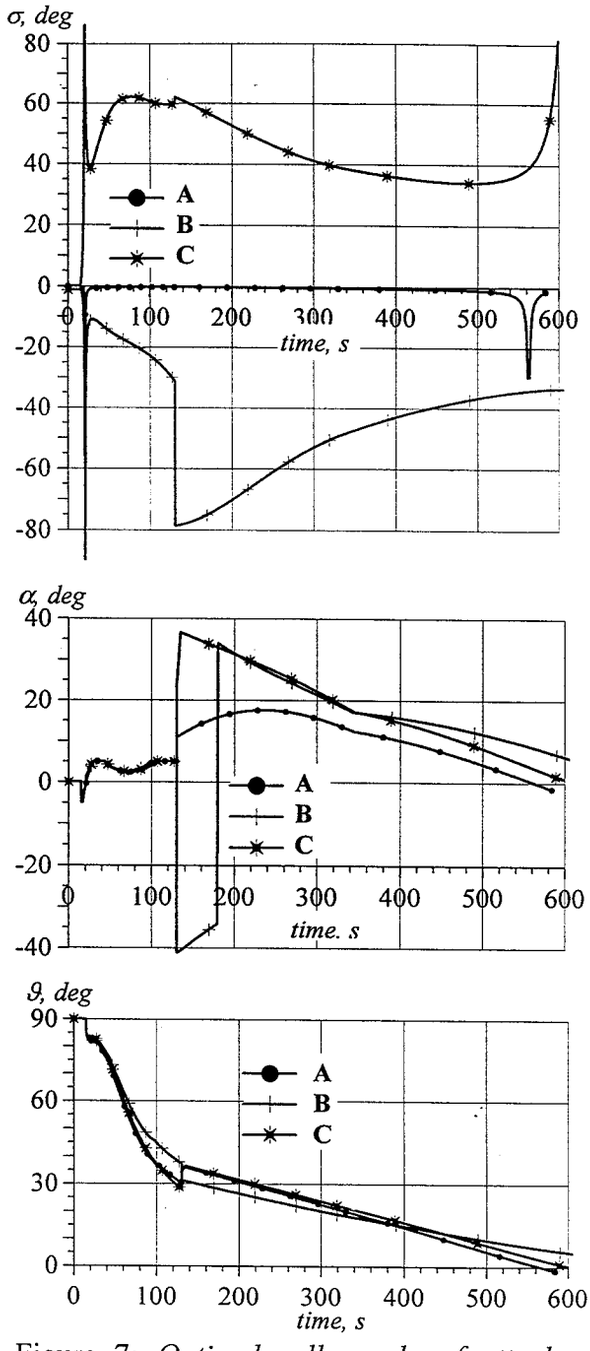

Figure 7: *Optimal roll, angle of attack and pitch programs for the insertion trajectories with different fixed fall points (see A, B and C cases in Fig. 6).*

specified regions allows a qualitative improvement of the insertion flexibility because it provides any-direction launch. Indeed, the insertion orbit inclination can be chosen in this case not from several values but from a continuous set.

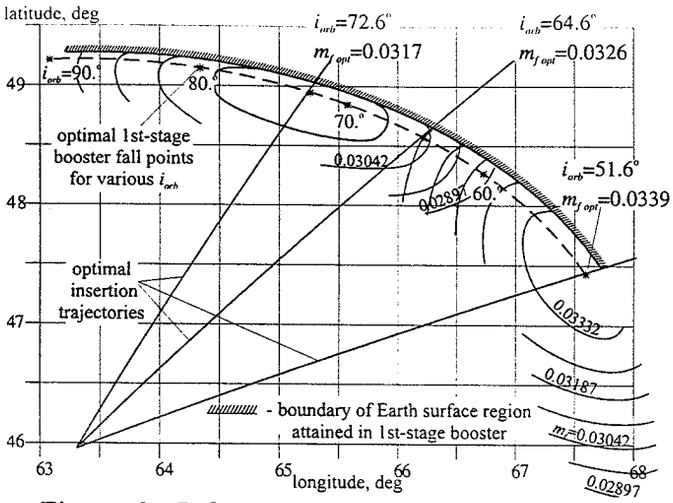

Figure 8: *Relative maximum mass m_f inserted into orbits with inclinations of i_{orb}=51.6° and 72.6° as a function of specified 1st-stage booster fall points.*

R-type launcher has 3 stages with initial mass ratios as 1:0.20:0.06. The control limitation on the 1st-stage is as $\alpha = 0$. The launcher is inserted into a circular orbit with a height of $h_{orb} = 295$ km and inclination of $i_{orb} = 51°$, the start point latitude being $\phi = 50°$.

A similar investigation through the use of the ASTER program complex is carried out for the optimal R-type launch vehicle injection when the spent 1st- and 2nd-stage boosters and the nose cover are dropped at specified Earth surface points.

Fig. 9 shows in the geographic coordinates (longitude-latitude) the boundaries of the Earth surface regions attained by the spent 1st-stage booster for different admissible relative losses in the injected mass $\Delta\overline{m}_f$. Here, $\Delta\overline{m}_f$ is the ratio of the maximum injected mass change due to the limitation on the 1st-stage booster fall point, to the maximum mass injected into a specified orbit with a free 1st-stage booster fall point. The level lines

$$\Delta\overline{m}_f(\theta,\phi) = \text{const}, \qquad (20)$$

depicted in Fig. 9, if presented in the coordinates of the longitudinal and lateral distances from the launch plane, are essentially independent of the target orbit inclination.

A significant deformation of the level lines for inclinations close to the launch point latitude stems from the fact that there are two local extremals, very close in terms of the functional (within ~0.01%), which provide the injection into an orbit with a specified inclination but differ in the launch azimuth, i.e., the injection into the "ascending" or "descending" orbital portion (see[3]). When the inclinations are close to the launch point latitude, these extremals are located close to each other and the level lines (20) intersect for each extremal.

The similar regions of accessible fall points for the nose cover and the 2nd-stage booster are shown in Fig. 10.

Fig. 11 demonstrates losses of the relative maximum injected mass $\overline{m}_f(\overline{L}) = \dfrac{m_f(\overline{L})}{\max\limits_{\overline{L}} m_f}$

due to limitation on the relative distance $\overline{L} = L/L_{\max}$ of a fall point for the 1st- and 2nd-stage boosters and for the nose cover.

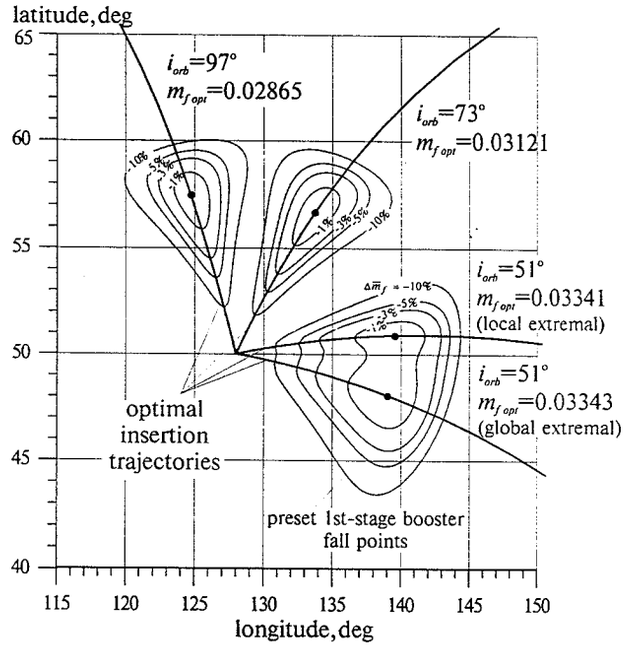

Figure 9: *Boundaries of the Earth surface regions attained by the spent 1st-stage booster for different admissible relative losses in the injected mass $\Delta\overline{m}_f$.*

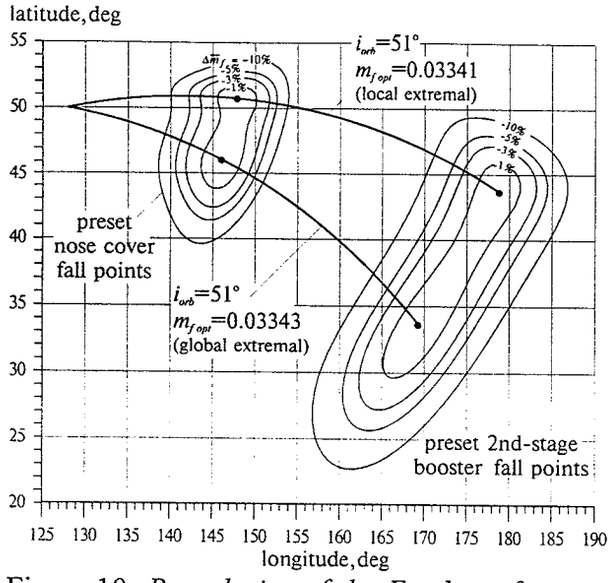

Figure 10: *Boundaries of the Earth surface regions attained by the spent nose cover and 2nd-stage booster for different admissible relative losses in the injected mass* $\Delta\overline{m}_f$.

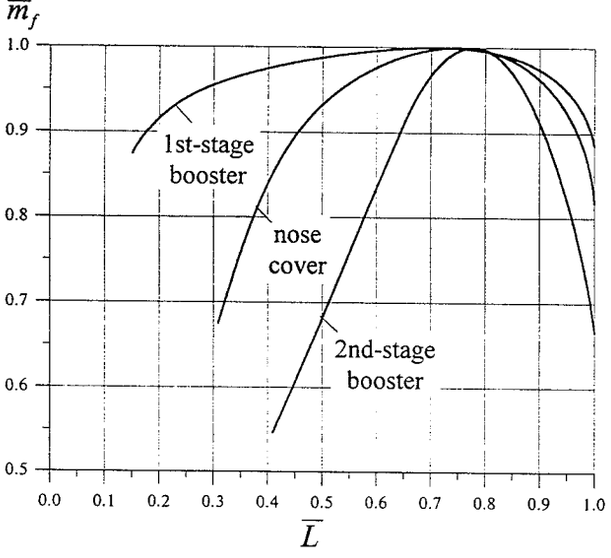

Figure 11: *The relative inserted mass* $\overline{m}_f$ *vs. the relative fall distance* $\overline{L}$ *of the 1st- and 2nd-stage boosters and nose cover.*

In principle, it is shown to be possible to provide such STS injection that the STS components, spent on different injection trajectory portions, fall at one and the same point. Fig. 12 illustrates the losses in the maximum injected mass $\overline{m}_f = \dfrac{m_f}{m_{f\,opt}}$, provided the condition that the 1st-stage booster and the nose cover fall at one and the same point, as a function of the distance L_I of the common fall point from the launch point. For comparison there are shown dependencies $\overline{m}_f(L)$ (dash lines) corresponding to solutions of two problems considered above: the first accounts for limitation on the 1st-stage booster range, and the second account for limitation on the nose cover range only.

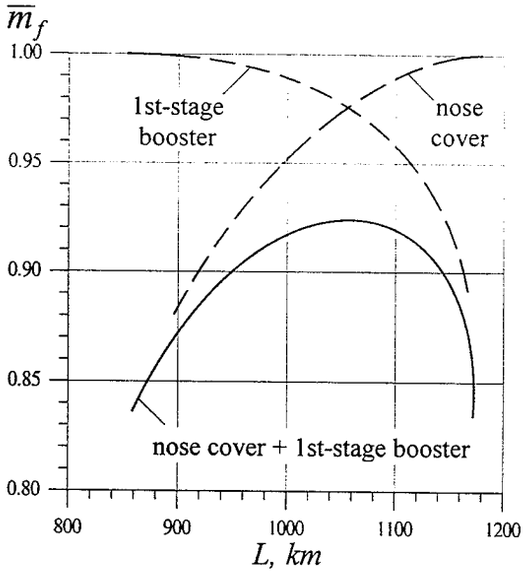

Figure 12: *The relative maximum inserted mass* $\overline{m}_f$ *vs. the range L of a common (the 1st-stage booster and the nose cover) fall point.*

Conclusions

The integration of the technology of the thorough optimization into the engineering practice of space vehicle designing enables the optimal injection trajectories to be formed both for advanced and existing STS based on the regular procedure with due regard for new requirements, limitations and control features. The application of the strict indirect optimization method of the Pontryagin's maximum principle type for branching processes in combination with the methods of the solution continuation and selection of local extremals, as is the case in the ASTER complex, guarantees the relevant automatic (without the investigator's interference) modification of the optimal control law structure, including that of the bifurcation type, resulted from the consideration for new factors,

if this improves the STS effectiveness. Similar capabilities are demonstrated by examples of solving the optimal injection problem for existing multi-stage STS with due regard for the limitation on fall zones for spent components (boosters and a nose cover).

It is shown the capability of:
- using unified alienation zones intended for vehicle injections into orbits in a wide range of orbit inclinations;
- varying the spent component fall point within the Earth surface region having the diameter comparable with the distance of the nominal fall point from the launch site;
- dropping STS components, used on different flight portions, at one and the same point, etc.

Of fundamental importance is the fact that when the optimal control laws are used, including nontraditional ones, the above-outlined capabilities can be realized with minimal losses of the injected mass.

References

1. D.E.Okhotsimskii and T.M.Eneev, *Some Variational Problems Connected With the Launching of Artificial Earth Satellites*, Usp. Fiz. Nauk, 63, No.1a, 5 (1957).
2. D.E.Lawden. *Optimum Trajectories for Space Navigation*, Butterworths, London (1963).
3. A.S.Filatyev, *Optimization of Spacecraft Ascent Using Aerodynamic Forces*, IAF-92-0022. The 43rd IAF Congress, 1992, Washington, DC.
4. L.S.Pontryagin, V.G.Boltyanskii, R.V.Gamkrelidze, and E.F.Mishchenko, *Mathematical Theory of Optimum Processes*, Nauka, Moscow (1969).
5. A.S.Filatyev, *Optimization of Branched Trajectories for Aerospace Transport Systems,* ICAS-94-5.5.3. The 19th ICAS Congress, 1994, Los Angeles.